Amino Acids (2014) 46:2531–2543
DOI 10.1007/s00726-014-1802-3

ORIGINAL ARTICLE

Design and characterization of short antimicrobial peptides using leucine zipper templates with selectivity towards microorganisms

Aqeel Ahmad · Sarfuddin Azmi · Saurabh Srivastava · Amit Kumar · Jitendra Kumar Tripathi · Nripendra N. Mishra · Praveen K. Shukla · Jimut Kanti Ghosh

Received: 1 February 2014 / Accepted: 30 June 2014 / Published online: 29 July 2014

Abstract Design of antimicrobial peptides with selective activity towards microorganisms is an important step towards the development of new antimicrobial agents. Leucine zipper sequence has been implicated in cytotoxic activity of naturally occurring antimicrobial peptides; moreover, this motif has been utilized for the design of novel antimicrobial peptides with modulated cytotoxicity. To understand further the impact of substitution of amino acids at 'a' and/or 'd' position of a leucine zipper sequence of an antimicrobial peptides on its antimicrobial and cytotoxic properties four short peptides (14-residue) were designed on the basis of a leucine zipper sequence without or with replacement of leucine residues in its 'a' and 'd' positions with D-leucine or alanine or proline residue. The original short leucine zipper peptide (SLZP) and its D-leucine substituted analog, DLSA showed comparable activity against the tested Gram-positive and negative bacteria and the fungal strains. The alanine substituted analog (ASA) though showed appreciable activity against the tested bacteria, it showed to some extent lower activity against the tested fungi. However, the proline substituted analog (PSA) showed lower activity against the tested bacterial or fungal strains. Interestingly, DLSA, ASA and PSA showed significantly lower cytotoxicity than SLZP against both human red blood cells (hRBCs) and murine 3T3 cells. Cytotoxic and bactericidal properties of these peptides matched with peptide-induced damage/permeabilization of mammalian cells and bacteria or their mimetic lipid vesicles suggesting cell membrane could be the target of these peptides. As evidenced by tryptophan fluorescence and acrylamide quenching studies the peptides showed similarities either in interaction or in their localization within the bacterial membrane mimetic negatively charged lipid vesicles. Only SLZP showed localization inside the mammalian membrane mimetic zwitterionic lipid vesicles. The results show significant scope for designing antimicrobial agents with selectivity towards microorganisms by substituting leucine residues at 'a' and/or 'd' positions of a leucine zipper sequence of an antimicrobial peptide with different amino acids.

Keywords Antimicrobial peptides · Designer peptides · Cell selectivity · Lipid vesicles · Membrane depolarization · Localization of peptides onto membrane

Abbreviations

PBS	Phosphate buffered saline
FITC	Fluorescin isothiocyanate
Fmoc	*N*-(9-fluorenyl) methoxycarbonyl
DIC	Differential interference contrast
HPLC	High-performance liquid chromatography
ESI-MS	Electron spray ionization- mass spectrometry
ANS	8-Anilinonapthalene-1-sulfonic acid
DiS-C3-5	3,3′-Dipropylthiadicarbocyanine iodide

A. Ahmad and S. Azmi contributed equally to the work. S. Srivastava and A. Kumar contributed equally to the work.

Electronic supplementary material The online version of this article (doi:10.1007/s00726-014-1802-3) contains supplementary material, which is available to authorized users.

A. Ahmad · S. Azmi · S. Srivastava · A. Kumar · J. K. Tripathi · J. K. Ghosh (✉)
Molecular and Structural Biology Division, CSIR-Central Drug Research Institute, Sector 10, Jankipuram Extension, Sitapur Road, Lucknow 226 031, India
e-mail: jk_ghosh@cdri.res.in; jighosh@yahoo.com

N. N. Mishra · P. K. Shukla
Fermentation Technology Division, CSIR-Central Drug Research Institute, Sector 10, Jankipuram Extension, Sitapur Road, Lucknow 226 031, India

Introduction

Emergence of resistant microorganisms against conventional antibiotics demands the development of new antimicrobial molecules that can successfully neutralize these microorganisms. From the smallest organisms to human being including plant kingdom, they produce a variety of antimicrobial peptides for their self-protection (Brogden and Brogden; Giuliani and Rinaldi). These antimicrobial peptides mostly target the membrane of microorganisms in order to show their microbicidal activity though reports on the intracellular target of these peptides are also there (Cudic and Otvos 2002; Zasloff 2002; Yeaman and Yount 2003; Brogden 2005; Nicolas 2009). More importantly, in vitro experiments suggest that membrane-active antimicrobial peptides deform the morphology of the microorganisms by lysing their cell membrane within a short time (Ma et al. 2013; Zasloff 2002; Yeaman and Yount 2003; Brogden 2005; Ahmad et al. 2006). Therefore, it is believed that resistance against antimicrobial peptides is not easy to build up for the microorganisms and these peptides are considered as promising lead molecules for developing new antimicrobial drugs.

Usually antimicrobial peptides are cationic and amphipathic in nature and possesses a stretch of 12–60 amino acids (Hultmark 2003). Membrane permeabilizing property of peptides provides with positive as well as negative aspect with respect to converting them into potential antimicrobial drugs. In terms of positive aspect, it provides lesser chance to the microorganisms to develop resistance while at the negative side it gives lesser selectivity to the antimicrobial peptides towards bacterial and mammalian cell membranes. Though it has been proposed by many research groups that cationicity confer more antimicrobial property and hydrophobicity in cytotoxic activity, but this is not universal.

Earlier in several studies it has been shown that leucine zipper sequences, present in many naturally occurring antimicrobial peptides, are responsible for their self-aggregation properties which further promote the peptides-induced permeabilization of mammalian cell membrane and thus cytotoxicity against human cells. Further, it was shown that minor amino acid substitutions at 'a' and 'd' positions of the leucine zipper-like sequences in an antimicrobial peptide can drastically impair its cytotoxic properties (Azmi et al. 2013; Pandey et al. 2010, 2011; Asthana et al. 2004; Ahmad et al. 2006, 2009a).

To further evaluate how alterations of amino acid sequences in a leucine zipper-like sequences influence the biological, structural and functional properties of an antimicrobial peptide, four 14-residue peptides were designed synthesized and characterized. Of these peptides, the first one was designed by employing an amphipathic leucine zipper-like sequence as a template and in the other three peptides leucine residues at heptadic positions were replaced with alanine, D-leucine and proline residues. We observed that leucine containing (SLZP) model peptide was more hemolytic and it maximally disturbed the integrity of the tested mammalian cells or the mimetic lipid membrane than D-leucine (DLSA), alanine (ASA) and proline (PSA) containing peptides. Except PSA all three peptides namely, SLZP, DLSA, and ASA showed comparable activities against the tested Gram-positive and negative bacteria, while the activity of PSA was lesser against both kinds of bacteria in comparison to other peptides. In antifungal assays, PSA showed the least activity among these peptides. Structural and functional studies were performed to understand the basis of activity in these peptides.

Materials and methods

Materials

Rink amide MBHA resin (loading capacity, 0.63 mmol/g) and all the *N*-α Fmoc and side-chain protected amino acids were purchased from Novabiochem, Switzerland. Coupling reagents for peptide synthesis like 1-hydroxybenzotriazole (HOBT), *N*, *N*′-di-isopropylcarbodiimide (DIC), 1,1,3,3-tetramethyluronium tetrafluoroborate (TBTU) and *N*, *N*′-diisopropylethylamine (DIPEA) were purchased from Sigma, India while Dichloromethane, *N*, *N*′ dimethylformamide (DMF) and piperidine were of standard grades and procured from reputed local companies. Acetonitrile (HPLC grade) was procured from Merck, India whereas trifluoroacetic acid (TFA) was purchased from Sigma, India. Egg phosphatidylcholine (PC), egg phosphatidylglycerol (PG) and dimyristoyl phosphatidylethanolamine (PE) were procured from Northern Lipids Inc., Canada while cholesterol (Chol) was purchased from Sigma. 3,3′-Dipropylthiadicarbocyanine iodide (diS-C_3-5) and NBD (4-fluoro-7-nitrobenz-2-oxa-1, 3-diazole) -fluoride were purchased from Molecular probes (Eugene, OR). Tissue culture plates (CELLSTAR-Greiner bio-one GmbH, Germany, RPMI 1640 medium buffered with MOPS (3-[*N* morpholino]propanesulfonic acid) (Sigma-Aldrich Chemical Co., St. Louis, MO, USA), VersaMax microplate reader (Molecular devices, Sunnyvale, USA), SOFTmax Pro 4.3 Software (Molecular Devices, Sunnyvale, USA). Rests of the reagents were of analytical grade and procured locally; buffers were prepared in milli Q water.

Methods

Peptide synthesis and purification

Stepwise solid phase syntheses of all the peptides were carried out manually on rink amide MBHA resin utilizing the standard Fmoc chemistry, reported earlier (Pandey et al. 2010; Yadav et al. 2003; Asthana et al. 2004). These peptides were purified by HPLC using C18 reverse phase column by running linear gradient of acetonitrile (0.1 %TFA) in water (0.1 %TFA) starting from 10 % and ending at 80 % in 40 min. The purified peptides were ~95 % homogeneous as shown by HPLC (Azmi et al. 2013).

Preparation of small unilamellar vesicles (SUVs)

SUVs were prepared by a standard procedure (Ghosh et al. 1997; Yadav et al. 2003; Asthana et al. 2004; Ahmad et al. 2006) with required amounts of either of the PC/cholesterol (8:1 w/w), or PC/PG (3:1 w/w) by employing a bath-type sonicator (Laboratory Supplies Company, New York) as reported earlier (Pandey et al. 2010, 2011; Ahmad et al. 2006).

Hemolytic activity assay

Hemolytic activity of these peptides against human red blood cells (hRBCs) was assayed by a standard procedure as reported earlier (Subbalakshmi et al. 1999; Asthana et al. 2004). For this purpose, fresh human red blood cells (hRBCs), collected in the presence of an anti-coagulant from a healthy volunteer, were received from a malaria research group of our Institute which possesses ethical approval from the institutional ethics committee (CDRI/IEC/CEM/21-07-2010) for collecting human blood for research purpose. hRBCs were washed three times in PBS. Then each of the peptides, dissolved in water, was added to the suspension of hRBCs (6 % final in v/v) in PBS to the final volume of 200 µl and incubated at 37 °C for 35 min. The percentage of hemolysis of hRBCs in the presence of these peptides was calculated as described before (Pandey et al. 2010, 2011).

Assay of antibacterial activity of the peptides

The antibacterial activity of the peptides was assayed in LB medium under aerobic conditions. Different concentrations of each of the peptides, dissolved in water, were added in duplicate to 100 µL (final volume) of medium containing the inocula of the test organism (~10^5 CFU) in mid-logarithmic phase of growth and incubated for 16–18 h. The peptide's antibacterial activities, expressed as their MICs (the peptide concentration which results 100 % inhibition of microbial growth), were assessed by measuring the absorbance at 600 nm (Azmi et al. 2013; Pandey et al. 2010).

Antifungal activity assay of designed peptides

In vitro antifungal activity evaluations of all the prepared peptide were evaluated for their in vitro antifungal activity against S. *schenckii, T. mentagrophytes, A. fumigatus,* and *C. parapsilosis* (ATCC 22019). In this process, the minimum inhibitory concentration of compounds was tested according to the standard microbroth dilution technique as per NCCLS guidelines. Briefly, experiment have been performed in flat-bottomed 96-well tissue culture plates in RPMI 1640 medium buffered with MOPS (3-[*N*-morpholino] propanesulfonic acid) for fungal strains. Initial inocula of fungal were maintained at 1–5 × 10^3cells/mL. These plates were incubated in a moist chamber at 35 °C, and an absorbance at 492 nm was recorded on a VersaMax microplate reader after 48 h for *C. parapsilosis*, 72 h for *A. fumigatus* and *S. schenckii*, and 96 h for *T. mentagrophytes*. The MICs were determined as 90 % inhibition of growth with respect to the growth control as observed using SOFTmax Pro 4.3 Software.

Analysis of peptide-induced membrane damage of hRBCs and *E. coli*

Peptide-induced phospholipid asymmetry or damage of phospholipid membrane organization of hRBCs was determined by staining the cells (final 0.6 % v/v in PBS) with FITC-annexin v after the treatment with the peptides at 37 °C for 5 min (Azmi et al. 2013; Ahmad et al. 2009a, 2009b). The hRBCs were then analyzed by flow cytometry in the form of dots plot with respect to the control cells not treated with any peptide. In order to check the membrane integrity of bacteria after peptide treatment, the cells at mid-log phase were incubated with peptides and for 30 and 60 min at 37 °C with constant shaking. The cells were centrifuged, washed two times with PBS, and incubated further with propidium iodide at 4 °C for 30 min, followed by removal of the unbound dye through washing with an excess of PBS and re-suspended in buffer. Peptide-induced damage of bacterial cells was then analyzed by a flow cytometer.

Tryptophan fluorescence studies of the peptides in the presence of lipid vesicles

All fluorescence measurements were performed in quartz cuvettes with 1-cm path length. And the fluorescence spectra were measured with a Perkin Elmer LS 55B

spectrometer with emission slit 8 nm and excitation slit set at 6 nm. The tryptophan residue of SLZP and analogs was excited at 280 nm, and emission spectra were recorded from 290 to 450 nm, averaging three scans. Spectra were recorded as a function of the lipid/peptide molar ratio. All Background signals of only lipid vesicles in buffer were subtracted from the corresponding spectra containing both lipid and peptide to minimize the contribution due to light scattering of lipid vesicles (Haldar et al. 2010). Blue shifts were calculated as the differences in wavelength of the maxima in emission spectra of lipid-peptide and peptide samples.

Quenching of Trp emission by acrylamide

To reduce absorbance by acrylamide, excitation of Trp at 295 nm instead of 280 nm was used (Weber and Shinitzky 1970; Gustiananda et al. 2004). Aliquots of the 3.0 M solution of this water-soluble quencher were added to the peptide in the absence or presence of liposomes at a peptide/lipid molar ratio of 1:100. The values obtained were corrected for dilution, and the scatter contribution was derived from acrylamide titration of a vesicle blank. The data were analyzed according to the Stern–Volmer equation (Azmi et al. 2013; Castellano and Lakowicz 1998; Bhunia et al. 2009).

$$F_0/F = 1 + K_{sv}[Q]$$

where F_0 and F represent the fluorescence intensities in the absence and the presence of the quencher (Q), respectively, and K_{sv} is the Stern–Volmer quenching constant, which is a measure of the accessibility of Trp to acrylamide. On the premise that acrylamide does not significantly partition into the membrane bilayer (Azmi et al. 2013), the value for K_{sv} can be considered to be a reliable reflection of the bimolecular rate constant for collisional quenching of the Trp residue present in the aqueous phase. Accordingly, K_{sv} is determined by the amount of nonvesicle-associated free peptide as well as the fraction of the peptide residing in the surface of the bilayer.

Analysis of peptide-induced membrane damage of hRBC's and *E. coli* cells by flow cytometry

Peptide-induced membrane damage of hRBC's cells was determined by staining the cells with annexin-V with FITC tagged after the treatment with the peptides at 37 °C for 15 min. These cells were then analyzed by flow cytometry in the form of dots plot with respect to the control cells, not treated with any peptide. In order to check the membrane integrity of bacteria after peptide treatment, the cells (*E. coli ATCC* 10536) at mid-log phase were incubated with peptides for 30 min and 60 min at 37 °C in two independent experiments with constant shaking. The cells were collected by centrifugation, washed two times with PBS, and incubated further with propidium iodide at 4 °C for 30 min, followed by removal of the unbound probe through washing with an excess of PBS and re-suspended in buffer. Peptide-induced damage of bacterial cells was then analyzed by flow cytometry.

Assay of peptide-induced depolarization of hRBC and *E. coli* cell membrane

Peptide-induced depolarization of hRBCs and *E. coli* ATCC 10536 membrane was detected by its efficacy to dissipate the potential across these cell membranes (Pandey et al. 2011; Papo et al. 2004; Yadav et al. 2008). Fresh human red blood cells (hRBCs) were collected in the presence of an anti-coagulant from a healthy volunteer and washed three times in PBS and re-suspended in the same buffer with a final cell density of $\sim 3.0 \times 10^7$ cells/ml. Human red blood cells were incubated with diS-C_3-5 probe for 1 h. When the fluorescence level (excitation and emission wavelengths set at 620 and 670 nm, respectively) of the hRBCs became stable, different amounts of each of the peptides were added to these suspensions and incubated at 37 °C for 30 min. After that peptide-induced membrane depolarization of human red blood cells were recorded. While the bacteria were grown at 37 °C until it reached to its midlog phase and centrifuged followed by washing with buffer (20 mM glucose, 5 mM HEPES pH 7.3). Then bacteria were resuspended (final $\sim 2 \times 10^5$ CFU/ml) in the similar buffer containing 0.1 M KCL) and incubated with diS-C_3-5 probe for 1 h. When the fluorescence level of bacterial suspension became stable, different amounts of each of the peptides were added to these suspensions to record the peptide-induced membrane depolarization of bacterial membrane. Membrane depolarization as measured by the fluorescence recovery (F_t) was defined by the equation (Pandey et al. 2011; Asthana et al. 2004; Ahmad et al. 2006; Sims et al. 1974; Loew et al. 1983; Yadav et al. 2003), $F_t = [(I_t - I_0)/(I_f - I_0)] \times 100$ %, where I_f, the total fluorescence, was the fluorescence levels of cell suspensions just after addition of diS-C_3-5; I_t, observed fluorescence after the addition of a peptide at a particular concentration either to hRBCs or to *E. coli* suspensions, which were already incubated with diS-C_3-5 probe for 1 h and I_0 is the steady fluorescence level of the cell suspensions after one hr incubation with the probe. Fluorescence was monitored at 670 nm with respect to time (s) with excitation wavelength of 620 nm. Excitation and emission slits were set at 8 and 6 nm, respectively.

Detection of calcein release from the calcein-entrapped lipid vesicles

Peptide-induced calcein release from calcein-entrapped lipid vesicles has been often employed to detect the pore-forming activity of proteins and peptides. Calcein-entrapped lipid vesicles were prepared with a self-quenching concentration (60 mM) of the dye in 10 mM HEPES at pH 7.4. The experimental methodology was the same as reported earlier (Allen and Cleland 1980; Yadav et al. 2003). Peptide-induced release of calcein from the lipid vesicles as measured by the fluorescence recovery is defined by the same equation as used to determine the peptide-induced depolarization of hRBC and bacteria or the dissipation of diffusion potential in lipid vesicles in the previous sections. However, in this case I_f, the total fluorescence, was determined after the addition of triton X-100 (0.1 % final concentration) to the dye-entrapped vesicle suspension. Excitation and emission slits were fixed 8 and 6 nm, respectively.

Circular dichroism experiments

CD spectra of the peptides were recorded in PBS, and in the presence of 40 % TFE (in water v/v) and 1 % SDS (in water w/v) by utilizing a Jasco J-810 spectropolarimeter. The samples were scanned at room temperature (~30 °C) in a capped quartz cuvette of 0.20 cm path length in the wavelength range of 250–195 nm. The fractional helicities were calculated with the help of mean residue ellipticity values at 222 nm by the following equation (Greenfield and Fasman 1969; Wu et al. 1981):

$$F_h = \frac{[\theta]_{222} - [\theta]^0_{222}}{[\theta]^{100}_{222} - [\theta]^0_{222}}$$

Assessment of binding of ANS to peptides

ANS (~20 μM) fluorescence was recorded in the presence of each of the peptides at ~47.0 μM concentration. The excitation wavelength and emission wavelength range for ANS were set at 365 and 410–600 nm (Azmi et al. 2013; Pandey et al. 2011; Javadpour and Barkley 1997). The excitation and emission slits were fixed at 6 and 4 nm, respectively.

Results

Design of peptides

The leucine residues positioned at 'a' and 'd' positions of a leucine zipper sequence contribute in the assembly of proteins or peptides by participating in the intermolecular side chain interactions. Thus the substitution of amino acids at 'a' and 'd' positions of a leucine zipper sequence present in an antimicrobial peptide provides a suitable way to introduce structural changes in it and then look into its implication in various properties of the molecule. In order to assess the impact of placing different amino acids at 'a' and 'd' positions of a leucine zipper sequence in an antimicrobial peptide, we have designed a 14-mer peptide with a leucine zipper sequence and its analogs that contain D-leucine, alanine and proline (Table 1) residues at these positions of the sequence. Leucine residues of the original short leucine zipper peptide (SLZP) at positions 4, 5 and 8 were substituted for the design of its three analogs; while 4 and 8 positions correspond to 'd' and 'a' positions respectively from the N-terminal of a heptad repeat sequence, position 5 correspond to an 'a' position if the heptad repeat sequence is counted from the first C-terminal

Table 1 Peptide designation, amino acid sequences, calculated and observed mass, and HPLC retention time of the designed peptides

Peptides Designation	Amino acids at a and d positions are bold and subsituted amino acids are bold and underlined (Italic L are D leucines)	Calculated Mass (Da)	observed mass (Da)	RP-HPLC retention times (min.)
	a b c d e f g a b c d e f g			
SLZP	L R R L L R W L R R L L R R	1975.47	1976	20.03
ASA	L R R A A R W A R R L L R R	1849.23	1848	10.3
DLSA	L R R *L L* R W *L* R R L L R R	1975.47	1976	15.2
PSA	L R R P P R W P R R L L R R	1927.34	1928	10.8

leucine residue (position 12 from the N-terminal). D-leucine, alanine and proline were chosen since these amino acids are recognized to impair the assembly/oligomeric properties of a protein when it is placed instead of a leucine at 'a' and/or 'd' position of the heptads (Suh et al. 1999; Ahmad et al. 2006; Zhu et al. 2007a). Furthermore, since these amino acids are also hydrophobic in nature, amphipathic property of the original peptide is retained in its analogs to a large extent.

SLZP and its analogs exhibited comparable and significant antimicrobial activity

To find out the antibacterial activity of SLZP and its analogs the peptides were tested for growth inhibiting activity in liquid cultures against Gram-positive and Gram-negative bacteria. Overall, there were not much differences between SLZP and ASA in activities against Gram-positive and negative bacteria (Table 2). However, PSA showed lower activity against these bacteria (Table 2). The results suggest that the antibacterial activity of SLZP remained nearly intact after the substitution of leucine residues by D-leucine and alanine residues against the tested Gram-positive or negative bacteria while the substitution with proline residues reduced the activity of SLZP. Antibacterial activities of these peptides were also evaluated in the presence of serum against one Gram-positive (*B. subtilis* ATCC 6633) and one Gram-negative (*E. Coli* ATCC 10536) bacteria. Antibacterial activity of all but one peptide, DLSA, was greatly affected in the presence of serum. The MIC values of DLSA in the presence of serum against *E. Coli* ATCC 10536 and *B. subtilis* ATCC 6633 were around double to that in the absence of serum, whereas SLZP and its other analogs exhibited their MIC values five to six times to that of the without serum (data not shown). The results suggest that serum protein inhibited the anti-bacterial activity of SLZP and its analogs against these selected bacteria to a varying degree and the substitutions with D-leucine residues inhibited the serum protein effect on bactericidal activity of SLZP significantly. However, in antifungal activity assays the alanine-substituted analog (ASA) showed moderate fungicidal activity against two fungal strains, *Sporothrix schenckii* and *Candida parapsilosis* (ATCC-22019) while proline substitution significantly reduced the activity of SLZP against all the tested fungal strains. The original leucine zipper peptide and its D-leucine substituted analogs showed comparable fungicidal activities against the four tested strains.

Table 2 Antimicrobial activity of the peptides

	Minimum inhibitory concentration (MIC) in μg/ml			
	SLZP	ASA	DLSA	PSA
Bacteria				
E. coli (ATCC 9637)	25	25	12.5	25
Pseudomonas aeruginosa (ATCC BAA-427)	25	25	12.5	100
Staphylococcus aureus (ATCC 25923)	1.56	3.15	3.15	12.5
Klebsiella pneumoniae (ATCC 27736)	3.15	6.25	6.25	12.5
B. cereus	3.15	3.15	3.15	>100
Fungi				
Sporothrix schenckii	3.15	12.5	6.25	100
Trichophyton mentagrophytes	6.25	100	12.5	>100
Aspergillus fumigatus	6.25	50	6.25	>100
Candida parapsilosis (ATCC-22019)	6.25	12.5	12.5	>100

Significant differences in cytotoxic activity of SLZP and its D-leucine, alanine and proline substituted analogs

Cytotoxic activity of SLZP and its analogs was determined by evaluating their hemolytic activity against the human red blood cells (hRBCs) and the viability of murine fibroblast cells (3T3) in their presence. Among the designed peptides SLZP was the most hemolytic; while the D-leucine-substituted analog was significantly less-hemolytic, the alanine and proline substituted analogs were almost non-hemolytic up to the tested 75 μM, peptide concentration against hRBCs (Fig. 1a).

Viability of 3T3 cells in the presence of SLZP and its analogs was evaluated by exploring the mitochondrial dehydrogenese activity of these cells by MTT assay. Similar to hemolytic activity assay, 3T3 cells were least viable in the presence of SLZP among these peptides. Also, the designed analogs DLSA, ASA and PSA exhibited a similar trend in cytotoxicity against the 3T3 cells (Fig. 1b) as was observed against the hRBCs. The results could be implicated to the role of leucine residues at 'a' and 'd' positions of the leucine zipper sequences in the cytotoxicity of these peptides which supports our previous observations (Azmi et al. 2013; Pandey et al. 2011; Ahmad et al. 2006, 2009b).

SLZP and its analogs potently damaged the membrane organization of bacteria cells but showed differences in mammalian cells

The changes in membrane organization of hRBC and bacteria, *E. coli,* in the presence of SLZP and its analogs was probed by incubating the peptide-treated cells with the mammalian lipid specific probe, annexin V, tagged with FITC and DNA-intercalating dye propidium iodide (PI), respectively. Phosphotidylserine predominantly present in

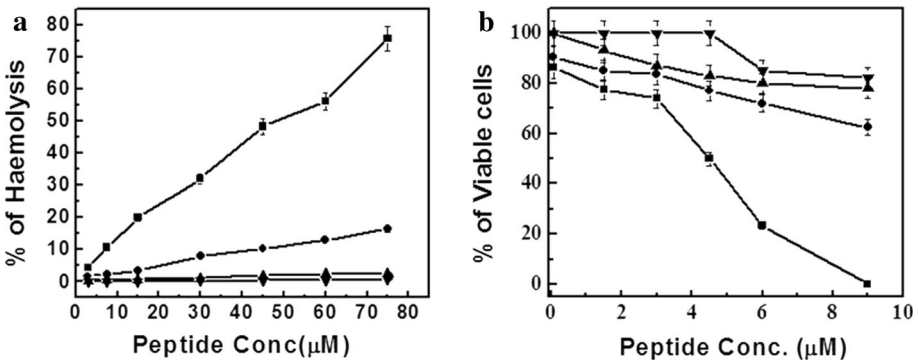

Fig. 1 Determination of cytotoxic activity of SLZP and its analogs. Dose-dependent hemolysis of hRBCs (**a**) and detection of viability of murine 3T3 cells (**b**) by MTT assay in the presence of SLZP and its analogs. Symbols: *solid square* SLZP; *solid circle* DLSA; *upright triangle* ASA; *inverted triangle* PSA. Each point represents the mean result of three independent experiments, and the error bar indicates the standard deviation

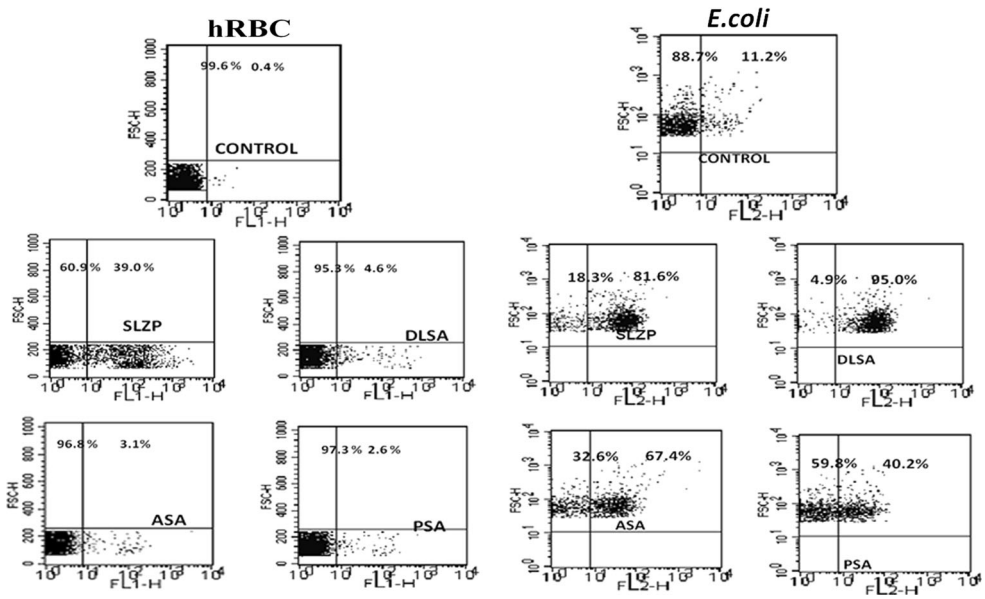

Fig. 2 Detection of peptide-induced perturbation of membrane organization of hRBCs and *E. coli* cells by flow cytometric studies. The panels in the *left-hand side* show the FITC annexin V staining of hRBCs without any peptide treatment (control), or treated with 30 μM concentration of SLZP or ASA or PSA or DLSA, as marked in the respective panel. The panels in the *right-hand side* show the PI staining of *E. coli* cells, without any peptide treatment (control) and treated with 6.0 μM concentration of SLZP, DLSA, ASA, and PSA as marked in the respective panel. On the *Y* axis, FSC-Height is forward scattered height which shows the distribution of the cells. In the *X* axis, FL1-Height means fluorescence recorded by fluorescent filter 1 (*green channel*) and FL2 means fluorescence recorded by fluorescent filter 2 (*red channel*). 10,000 events were counted for each experiment

inner leaflet of plasma membrane and annexin V-FITC is impermeable to normal mammalian cells. Annexin V binding to plasma membrane of peptide treated cells indicates peptide-induced damage of the mammalian cell membrane. SLZP treated hRBCs showed the maximum binding to FITC tagged annexin V than its analogs DLSA, ASA and PSA indicating the maximum damage of hRBC membrane organization by SLZP (Fig. 2).

On the other hand, interesting results were obtained when *E. coli* cells were stained with PI following the treatment with SLZP and its analogs. In contrast to annexin V binding to peptide-treated hRBCs, *E. coli* cells treated with either SLZP or its analogs for 60 min showed comparable entry of PI (Fig. 2). However, after 30 min treatment of cells with these peptides, only DLSA exhibited maximum transfer of the dots (68.0 %) to the upper right side of quadrant (Suppl. Figure 1) indicating PI staining of the membrane-damaged, bacteria. Results indicate that DLSA exhibited faster kinetics than other peptides in inducing membrane damage to the bacteria (Suppl.

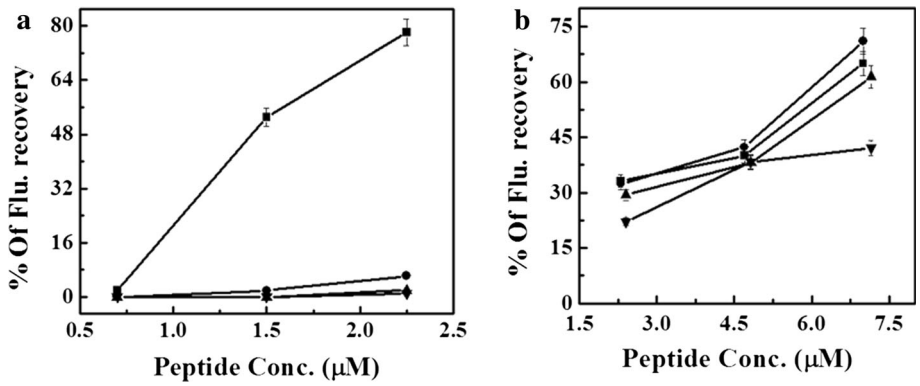

Fig. 3 Dose-dependent peptide-induced transmembrane depolarization of mammalian, hRBC and *E. coli* cells. *Left* and *right* panels show the plot of the percentage of fluorescence recovery, which is a measure of transmembrane depolarization, versus peptide concentration in hRBC and *E. coli* cells, respectively; symbols: *solid square* SLZP, *solid circle* DLSA, *upright triangle* ASA, *inverted triangle* PSA

Figure 1). Altogether the data disclose that the substitution of leucine by D-leucine, alanine and proline at the 'a' and 'd' positions of the leucine zipper sequence of SLZP impairs the ability of the peptide to damage the membrane organization of hRBCs but not bacteria.

SLZP and its analogs depolarized hRBC membrane to a different extent while comparable depolarization of *E. coli* membrane was observed in the presence of these peptides

Membrane depolarization of *E. coli* and hRBCs was evaluated in the presence of SLZP and its analogs in order to make out their probable mode of action and the basis of their contrasting cytotoxicity but comparable bactericidal activity. SLZP and its analogs excluding PSA, induced a comparable extent of depolarization in *E. coli* cell membrane; PSA induced relatively lesser depolarization ($\approx$25 %) than the other peptides of this group (Fig. 3). Nevertheless, SLZP was much more active in comparison to its analogs in depolarizing hRBC membrane which was consistent to its cytotoxicity and hRBC membrane depolarization induced by other peptides also match with their hemolytic activity (Fig. 1a). The results all together show a significant effect of substitution of leucine residues at 'a' and 'd' positions of leucine zipper sequence on the SLZP-induced depolarization of hRBCs, however, it showed much less effect on the peptide-induced depolarization of *E. coli* membrane.

Differences among the peptides in permeabilizing the mammalian membrane mimetic lipid vesicles but not in bacterial cell membrane mimetic lipid vesicles

Zwitterionic (like PC/Chol) and negatively charged (like PE/PG or PC/PG) lipid vesicle are employed as mimetics of eukaryotic and prokaryotic cell membrane, respectively. To examine SLZP and its analogs induced permeabilization of zwitterionic and negatively charged lipid vesicles, peptide-induced calcein release from calcein-entrapped both kinds of lipid vesicles were studied. SLZP and its analogs DLSA and ASA appreciably induced the leakage of calcein from calcein-entrapped negatively charged PC/PG (7:3, w/w) lipid vesicles while PSA caused relatively lesser leakage of calcien as evidenced by the representative calcein release profiles (Fig. 4a) and plot of fluorescence recovery data (Fig. 4c). On other hand, DLSA, ASA and PSA induced significantly lesser calcien leakage from zwitterionic calcein-entrapped PC/Cholesterol lipid vesicles than SLZP (Fig. 4b, d). Like the peptide-induced depolarization of hRBC and *E. coli* membrane, data of permeabilization of zwitterionic and negatively charged lipid vesicles in the presence of SLZP and its analogs match with their relative cytotoxicity and bactericidal properties, respectively.

Differences among the peptides in interacting with zwitterionic lipid vesicles but not with negatively charged lipid vesicles

The sensitivity of the fluorescence emission of the Tryptophan residue to its environment allows us to monitor the binding of peptides to different membrane mimetic lipid vesicles. Tryptophan emission maxima of SLZP shifted significantly towards the shorter wavelength in the presence of zwitterionic lipid vesicles as compared to that in PBS (Fig. 5a). On the other hand, emission maxima of SLZP analogs did not shift appreciably towards the shorter wavelength in the presence of the zwitterionic lipid vesicles, except the emission maxima of DLSA shifted to some extent towards the shorter wavelength indicating relatively stronger binding with the mammalian membrane mimetic lipid vesicles in comparison to the other SLZP-analogs. However, in the presence of negative charged lipid vesicles except DLSA Tryptophan emission maxima of all peptides significantly shifted towards shorter wavelength as compared to that in PBS (Fig. 5b). The results indicate that unlike in zwitterionic lipid vesicles, tryptophan residues of

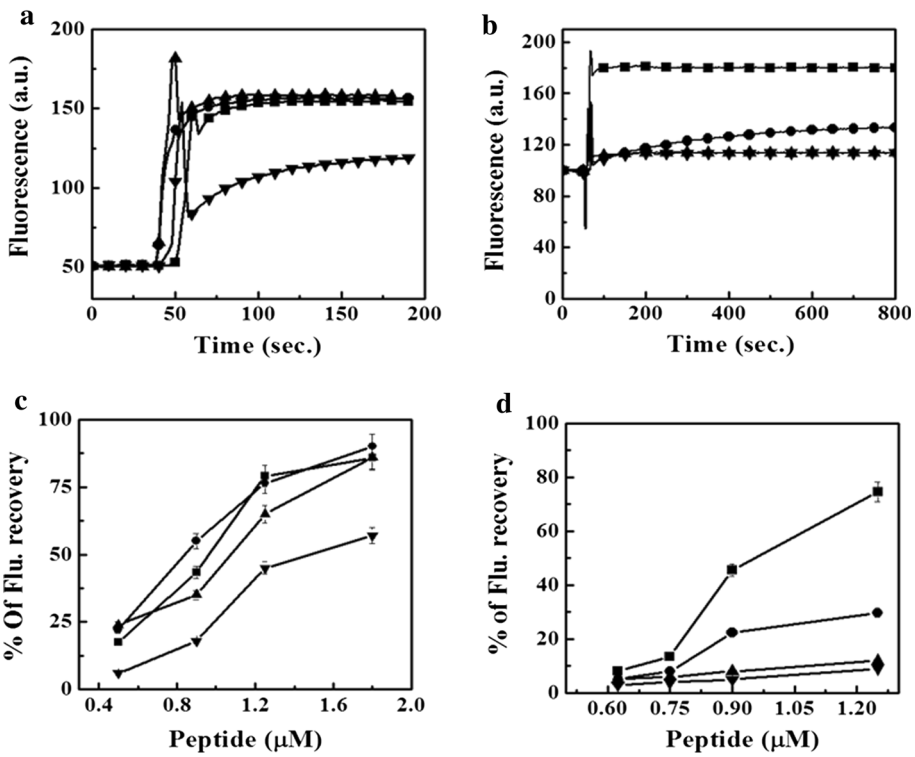

Fig. 4 Determination of peptides-induced permeabilization of mimetic model membranes by studying the peptide-induced release of calcein from calcein-entrapped different kinds of lipid vesicles. **a**, **b** show the experimental profiles of calcein release induced by SLZP and its analogs from calcein-entrapped negatively charged and zwitterionic lipid vesicles, respectively. Concentration of each peptide in **a** and **b** were 1.8 and 1.25 μM, respectively. **c**, **d** show the plots of peptide-induced fluorescence recovery of calcein release from PC/PG [7:3 (w/w)] and zwitterionic, PC/Chol [8:1 (w/w)] lipid vesicles respectively. Symbols: *solid square* SLZP; *solid circle* DLSA; *upright triangle* ASA; *inverted triangle* PSA

ASA and PSA were localized in the hydrophobic core of the negatively charged lipid vesicles similar to the SLZP. However, probably the substitutions of leucine residues by D-leucine residues altered the conformation of SLZP in such a way that its tryptophan residue did not enter into the hydrophobic environment of the negatively charged lipid vesicles (Fig. 5).

Examination of localization of tryptophan residue of the peptides when bound to the zwitterionic and negatively charged lipid vesicles

The observed changes in the characteristics of tryptophan emission maximum upon binding of these peptides to lipid vesicles indicate the localization of the tryptophan residue of a particular peptide to the nature of environment of the corresponding phospholipid membrane. Acrylamide was used as a quencher of tryptophan fluorescence to further investigate the localization of the tryptophan residue of SLZP and its analogs when these peptides are bound to different kinds of lipid vesicles. This neutral, water-soluble quencher has the advantage that no electrostatic interactions take place with the head group of negatively charged phospholipids and it. Tryptophan fluorescence of these peptides decreased in a concentration-dependent manner with addition of acrylamide to the peptide solution both in the absence and presence of lipid vesicles. However, in the presence zwitterionic lipid vesicles least decrease of Trp emission took place for SLZP followed by DLSA, ASA and PSA with increasing concentration of acrylamide suggesting the accessibility of the tryptophan residue of the peptides to acrylamide when bound to zwitterionic lipid vesicles follows the order SLZP $\ll$ DLSA $<$ ASA $\ll$ PSA (Fig. 5c). Nevertheless, in the presence of negatively charged lipid vesicles all the peptides exhibited comparable extent of quenching of tryptophan fluorescence with increasing concentration of the quencher (Fig. 5d, closed symbols); however, as expected the maximum quenching of fluorescence in the presence of acrylamide was observed when the peptides were in PBS (Fig. 5d, open symbols). The results could be implicated towards the differences in the localization of tryptophan residue of these peptides when they are bound to zwitterionic lipid vesicles and similar localization of their tryptophan residues when bound to the negatively charged lipid vesicles.

Distinct self-aggregation property of SLZP and its analogs in aqueous environment

ANS-(1-anilino-8-naphthalene sulfonate) anion is effectively bound to cationic groups of water-soluble proteins and polyamino acids through ion pair formation (Matulis et al. 1999). However, in hydrophobic milieu its fluorescence enhances significantly with shift of its emission maximum towards a shorter wavelength (Bolognesi et al. 2010). Thus self-association or aggregation of peptides in aqueous environment can be monitored by employing such

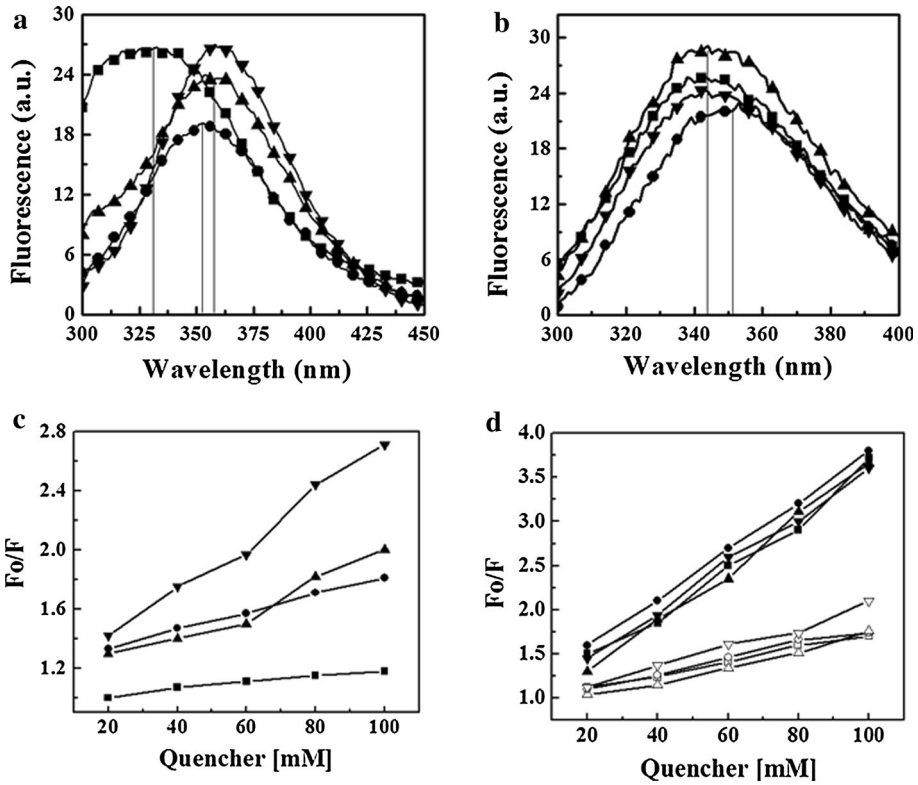

Fig. 5 Determination of environment of the tryptophan residues of SLZP and its analogs in their membrane-bound states by recording their emission maxima and by the Stern–Volmer plots of acrylamide quenching of their tryptophan fluorescence in the presence of different lipid vesicles. **a** and **b** depict the fluorescence spectra of the peptides in zwitterionic, PC/Chol and negatively charged, PC/PG lipid vesicles, respectively. **c** shows the Stern–Volmer plots for the acrylamide quenching of tryptophan fluorescence of these peptides in the presence of zwitterionic, PC/Chol lipid vesicles, while in **d** solid and *open symbols* show the same plot for the peptides in the presence of negatively charged lipid vesicles and in PBS, respectively. *Symbols* in **a**, **b**, **c** and **d**: *solid square*, SLZP; *solid circle*, DLSA; *solid upright triangle*, ASA and *solid inverted triangle*, PSA; Symbols for Stern–Volmer plots of peptides in PBS in **d**: *open square* SLZP; *open circle* DLSA; *open upright triangle*, ASA and *open inverted triangle*, PSA

kind of probe which can fluoresce in hydrophobic milieu. In PBS ANS showed negligible fluorescence, while in the presence of SLZP fluorescence of ANS increased significantly with emission maximum at shorter wavelength at ~480 nm, indicating the association of the probe to the hydrophobic environment of the peptide possibly due to its aggregation (Suppl. Figure 2). Interestingly, a totally distinct result was observed when ANS fluorescence was recorded in the presence of SLZP analogs. D-Leucine substituted analogs showed much lesser enhancement of ANS fluorescence and almost negligible shift of emission maximum toward the shorter wavelength as compared to that observed for the parent molecule, SLZP (Suppl. Figure 2); while other analogs ASA and PSA did not induce any enhancement and blue shift in fluorescence of ANS. The data clearly indicated that SLZP was much more self-aggregated than its other analogs in aqueous environment. Despite having the same amino acid composition as SLZP, DLSA did not aggregate as the parent peptide.

Secondary structures of SLZP and its analogs in different kinds of lipid vesicles

To determine secondary of SLZP and its analogs circular dichroism experiments were performed in aqueous buffer (PBS, pH 7.4), and zwitterionic and negatively charged lipid vesicles (Fig. 6). None of the peptides adopted any helical structure in aqueous milieu (profile not shown). SLZP adopted helical secondary structure in zwitterionic, PC/Chol lipid vesicles, whereas ASA showed a shoulder at ~220 nm instead of a prominent peak, characteristic of α-helical structure, suggesting a lack of proper helical structure of this peptide in this environment. CD spectrum of DLSA did not show the presence of significant secondary structure in PC/Chol lipid vesicles.

On the other hand, interestingly, in the presence of negatively charged PC/PG lipid vesicles, SLZP, ASA and DLSA adopted mostly α-helical structure. CD spectra of PSA in both PC/Chol and PC/PG lipid vesicles (Fig. 6a, b)

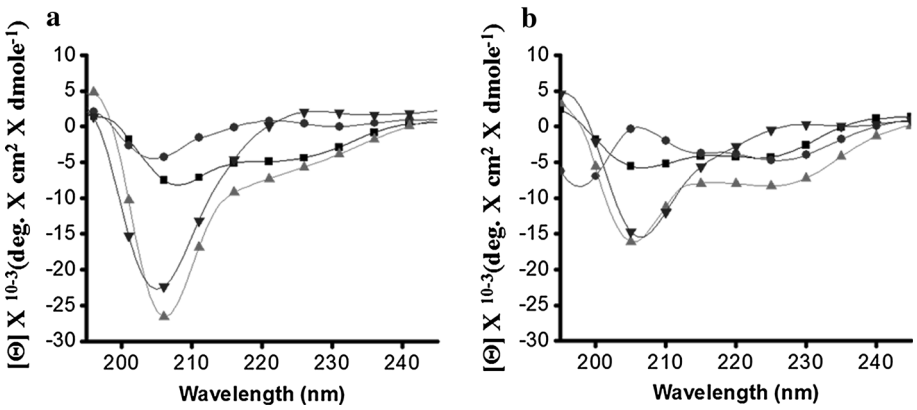

Fig. 6 Determination of secondary structures of SLZP and analogs (~28 μM) in zwitterionic–PC/Chol (**a**) and anionic PC/PG (**b**) lipid vesicles. Spectra of peptides are represented by symbols: *square* SLZP, *circle* DLSA, *upright triangle* ASA and *inverted triangle* PSA. Concentration of lipid vesicles was ~132 μM in both set of experiments, respectively

probably suggest the presence of weak β-turn structure (Crisma et al. 1984).

Discussion

It has already been demonstrated that leucine/isoleucine/phenylalanine zipper sequence plays a significant role in determining cytotoxicity rather than antimicrobial activities in naturally occurring or synthetic peptides (Azmi et al. 2013; Pandey et al. 2011; Zhu et al. 2007b) that possess any of these structural elements. The current study also confirms our previous observations since the substitution of leucine by D-leucine, alainine or proline drastically reduced their cytotoxicity against mammalian cells (Fig. 1). In previous studies (Pandey et al. 2011; Ahmad et al. 2006, 2009a) the leucine/isoleucine/phenylalanine residues at 'a' and 'd' positions of a leucine/isoleucine/phenylalanine zipper containing antimicrobial peptide were replaced by alanine residues. Looking at the importance of the amino acids at these positions in assembly and cytotoxicity of the antimicrobial peptides having leucine zipper-like sequences, it was of interest to investigate the impact of substitutions of leucine residues at these positions with diastereomeric leucine and proline residues. Though substitution of leucine residues with alanine residues significantly retained the activity of SLZP against the tested bacteria, a decline in activity is prominent following the substitutions of three leucine residues with three proline residues (Table 2). Since proline is even less hydrophobic than alanine, the data probably signify the requirement of sufficient hydrophobicity of the peptide in permeabilizing the bacterial membrane. The results support our earlier studies as well as many studies in the literature (Azmi et al. 2013; Chen et al. 2007). Decline in bactericidal activity in the presence of serum indicates the interference of plasma proteins with activity of antimicrobial peptides as observed for other AMPs also (Deslouches et al. 2005; Varkey and Nagaraj 2005). But lesser interference of plasma protein on the bactericidal activity of DLSA as compared to other peptides of this set, suggests that non-natural amino acids substituted peptides could be of interest for in vivo system. The fungicidal activity data of the peptides, particularly, the reduced activity of ASA and PSA and higher antifungal activity of SLZP and DLSA suggest that hydrophobicity of the peptides could have greater role in determining their activity against these tested fungal strains which is also supported by the data in the literature (Jiang et al. 2008). However, higher hydrophobicity may compromise with the cytotoxicity of an antimicrobial peptide. Therefore, it is challenging to design an antifungal peptide with low cytotoxicity. Results obtained with the leucine zipper based natural or designed antimicrobial peptides provide valuable information in this regard. As evident from the previous studies (Asthana et al. 2004; Ahmad et al. 2006) and the present study, substitution of amino acids at 'a' and/or 'd' position(s) is enough for reducing cytotoxicity of such peptides. Therefore, substitution of leucine/isoleucine residues at such positions with a hydrophobic amino acid which is also capable of altering the assembly of the leucine zipper peptide like in the present study, D-leucine residues, could probably retain the anti-fungal activity of the parent antimicrobial peptide with simultaneous reduction in its cytotoxicity.

Our detailed studies on ability of the peptides to damage the membrane organization (Fig. 2) or depolarize representative mammalian and bacterial membrane (Fig. 3) or permeabilize the both kinds of mimetic lipid vesicles (Fig. 4) suggest that these peptides probably interact with the membrane of target cell to show their activity. More importantly, the membrane-permeabilization properties of these peptides match with their biological activity also. Moreover, membrane permeabilization properties of SLZP and its analogs match with their interaction and localization onto different kinds of mimetic lipid vesicles (Fig. 5).

CD studies in the presence of zwitterionic lipid vesicles (Fig. 6) showed helical structure of SLZP. As already mentioned substitution of leucine residues at 'a' and/or 'd' position(s) by alanine residues disturbs the helical self-

assembly of leucine zipper containing peptides and there are several reports on abrogation of helical structures of antimicrobial peptides in the presence of zwitterionic vesicles following similar substitutions (Pandey et al. 2011; Ahmad et al. 2006) which was also observed in the current study. However, ASA adopted appreciable helical structure in negatively charged lipid vesicles (Fig. 6b). Diastereomeric amino acid substitutions usually alter the helix sense of a peptide; we presume that the substitutions of three L-leucine residues by its diastereomer could impair its helix sense as well as its helical assembly. Interestingly, though DLSA did not adopt significant secondary structure in zwitterionic lipid vesicles, it showed appreciable secondary structure in the presence of negatively charged lipid vesicles. Introduction of proline residues in SLZP showed the presence of weak β-turn structure.

In our recent study, biological properties of antimicrobial peptides (Azmi et al. 2013) designed on the basis of heptad repeat sequence with different hydrophobic residues at 'a' and 'd' positions were studied. However, the effects of substitution of leucine residues at 'a' and 'd' positions with its diastereomer or a helix breaking amino acid like, proline that have been studied here were not attempted previously (Azmi et al. 2013). Cytotoxic antimicrobial peptides mostly exhibit helical structures in mammalian membrane mimetic zwitterionic lipid vesicles suggesting that these peptides probably need such structure in order to form membrane lytic pores in mammalian membrane (Shai 1999; Asthana et al. 2004). The previous (Azmi et al. 2013; Pandey et al. 2011; Asthana et al. 2004; Ahmad et al. 2006) as well as the present study suggest that 'a' and 'd' positions of the leucine zipper-like sequences are crucial at which amino acid substitutions could impair the secondary structures of such peptides in zwitterionic lipid vesicles and thus determine their interaction with this kind of lipid vesicles as well as mammalian cell membrane whose outer layer is composed of such lipids. Evidently, except SLZP other peptides show lower helical structures in zwtter ionic lipid vesicles (Fig. 6) which match with their cytotoxicity. Thus structure–function studies on leucine zipper based antimicrobial peptides provide valuable information for controlling the interaction of such peptides with mammalian membrane mimetic lipid vesicles or mammalian membrane.

The results presented here suggest that substitutions with diastereomeric leucine (DLSA) and proline residues (PSA) also impaired the cytotoxic activity of short leucine zipper containing peptide, SLZP. Moreover, DLSA showed faster kinetics in damaging the membrane organization of the examined bacteria (Suppl. Figure 1) which could be a positive point in favor of replacing leucine by D-leucine residues at these characteristic positions. Weaker hemolytic activity of DLSA and PSA is supported by their weaker efficacy to damage the membrane organization of human red blood cells and permeabilize the mammalian membrane mimetic zwitterionic lipid vesicles. Further, DLSA and PSA also showed significantly weaker self-assembly properties in aqueous environment suggesting that both the diastereomeric leucine and helix breaking proline residues disturb the self-association property of SLZP in aqueous buffer (Suppl. Fig. 2). Though both ASA and PSA showed poor cytotoxic activity and both did not adopt appreciable secondary structures in zwitterionic membrane, significant differences were observed between these two peptides in negatively charged lipid vesicles (Fig. 6). In contrast to ASA which adopted appreciable helical structure in bacterial membrane mimetic negatively charged lipid vesicles, PSA did not show any significant helical structure in this environment. The data signify the weaker helix propensity of PSA, which could also contribute in its poor antimicrobial property. The data further show the importance of both hydrophobicity and secondary structure of these peptides for their antimicrobial properties. It is to be mentioned that even after substitutions of three leucine residues with three alanine residues in this short 14-residue peptide, ASA showed significant antimicrobial property probably suggesting that only hydrophobicity does not control the antimicrobial properties of a peptide and certain amount of compromise in hydrophobic property of a peptide does not necessarily alter its antimicrobial properties.

Altogether the results presented here show design and characterization of cell-selective antimicrobial peptides by utilizing an amphipathic leucine zipper-like sequence. The data show further scope for design of novel antimicrobial molecules using leucine zipper templates with selective activity towards microorganisms by introducing different amino acids at 'a' and 'd' positions of such sequences.

Acknowledgments CSIR-CDRI communication number of this manuscript is 8728. We are extremely grateful to Dr. S. K. Puri, Parasitology Division, CSIR-CDRI for kindly providing us fresh hRBCs for performing hemolytic activity assays with our peptides. The work was supported by the CSIR network projects NWP 0005 and BioDiscovery (BSC 0120). AA, SA, SS acknowledges the receipt of senior research fellowships from Council of Scientific and Industrial Research (CSIR), India; AK and JKT receipt of senior research fellowships from ICMR and UGC. The authors are extremely thankful to AL Vishwakarma for recoding the flow cytometry profiles and Sanjeev Kanojiya, Sophisticated Analytical Instrumentation Facility (SAIF), CSIR-CDRI for recording the ES-MS mass spectra.

Conflict of interest The authors declare that they do not have any conflict of interest.

References

Ahmad A, Yadav SP et al (2006) Utilization of an amphipathic leucine zipper sequence to design antibacterial peptides with simultaneous modulation of toxic activity against human red blood cells. J Biol Chem 281(31):22029–22038

Ahmad A, Asthana N et al (2009a) Structure-function study of cathelicidin-derived bovine antimicrobial peptide BMAP-28: design of its cell-selective analogs by amino acid substitutions in the heptad repeat sequences. Biochim Biophys Acta 1788(11):2411–2420

Ahmad A, Azmi S et al (2009b) Design of nontoxic analogues of cathelicidin-derived bovine antimicrobial peptide BMAP-27: the role of leucine as well as phenylalanine zipper sequences in determining its toxicity. Biochemistry 48(46):10905–10917

Allen TM, Cleland LG (1980) Serum-induced leakage of liposome contents. Biochim Biophys Acta 597(2):418–426

Asthana N, Yadav SP et al (2004) Dissection of antibacterial and toxic activity of melittin: a leucine zipper motif plays a crucial role in determining its hemolytic activity but not antibacterial activity. J Biol Chem 279(53):55042–55050

Azmi S, Srivastava S et al (2013) Characterization of antimicrobial, cytotoxic, and antiendotoxin properties of short peptides with different hydrophobic amino acids at "a" and "d" positions of a heptad repeat sequence. J Med Chem 56(3):924–939

Bhunia A, Mohanram H et al (2009) Lipopolysaccharide bound structures of the active fragments of fowlicidin-1, a cathelicidin family of antimicrobial and antiendotoxic peptide from chicken, determined by transferred nuclear Overhauser effect spectroscopy. Biopolymers 92(1):9–22

Bolognesi B, Kumita JR et al (2010) ANS binding reveals common features of cytotoxic amyloid species. ACS Chem Biol 5(8):735–740

Brogden KA (2005) Antimicrobial peptides: pore formers or metabolic inhibitors in bacteria? Nat Rev Microbiol 3(3):238–250

Brogden NK, Brogden KA (2011) Will new generations of modified antimicrobial peptides improve their potential as pharmaceuticals? Int J Antimicrob Agents 38(3):217–225

Castellano FN, Lakowicz JR (1998) A water-soluble luminescence oxygen sensor. Photochem Photobiol 67(2):179–183

Chen Y, Guarnieri MT et al (2007) Role of peptide hydrophobicity in the mechanism of action of alpha-helical antimicrobial peptides. Antimicrob Agents Chemother 51(4):1398–1406

Crisma M, Fasman GD et al (1984) Peptide models for beta-turns. A circular dichroism study. Int J Pept Protein Res 23(4):411–419

Cudic M, Otvos L Jr (2002) Intracellular targets of antibacterial peptides. Curr Drug Targets 3(2):101–106

Deslouches B, Islam K et al (2005) Activity of the de novo engineered antimicrobial peptide WLBU2 against *Pseudomonas aeruginosa* in human serum and whole blood: implications for systemic applications. Antimicrob Agents Chemother 49(8):3208–3216

Ghosh JK, Ovadia M et al (1997) A leucine zipper motif in the ectodomain of Sendai virus fusion protein assembles in solution and in membranes and specifically binds biologically-active peptides and the virus. Biochemistry 36(49):15451–15462

Giuliani A, Rinaldi AC (2011) Beyond natural antimicrobial peptides: multimeric peptides and other peptidomimetic approaches. Cell Mol Life Sci 68(13):2255–2266

Greenfield N, Fasman GD (1969) Computed circular dichroism spectra for the evaluation of protein conformation. Biochemistry 8(10):4108–4116

Gustiananda M, Liggins JR et al (2004) Conformation of prion protein repeat peptides probed by FRET measurements and molecular dynamics simulations. Biophys J 86(4):2467–2483

Haldar S, Raghuraman H et al (2010) Membrane interaction of the N-terminal domain of chemokine receptor CXCR1. Biochim Biophys Acta 1798(6):1056–1061

Hultmark D (2003) Drosophila immunity: paths and patterns. Curr Opin Immunol 15(1):12–19

Javadpour MM, Barkley MD (1997) Self-assembly of designed antimicrobial peptides in solution and micelles. Biochemistry 36(31):9540–9549

Jiang Z, Kullberg BJ et al (2008) Effects of hydrophobicity on the antifungal activity of alpha-helical antimicrobial peptides. Chem Biol Drug Des 72(6):483–495

Loew LM, Rosenberg I et al (1983) Diffusion potential cascade. Convenient detection of transferable membrane pores. Biochemistry 22(4):837–844

Ma QQ, Lv YF et al (2013) Rational design of cationic antimicrobial peptides by the tandem of leucine-rich repeat. Amino Acids 44(4):1215–1224

Matulis D, Baumann CG et al (1999) 1-Anilino-8-naphthalene sulfonate as a protein conformational tightening agent. Biopolymers 49(6):451–458

Nicolas P (2009) Multifunctional host defense peptides: intracellular-targeting antimicrobial peptides. FEBS J 276(22):6483–6496

Pandey BK, Ahmad A et al (2010) Cell-selective lysis by novel analogues of melittin against human red blood cells and *Escherichia coli*. Biochemistry 49(36):7920–7929

Pandey BK, Srivastava S et al (2011) Inducing toxicity by introducing a leucine-zipper-like motif in frog antimicrobial peptide, magainin 2. Biochem J 436(3):609–620

Papo N, Braunstein A et al (2004) Suppression of human prostate tumor growth in mice by a cytolytic D-, L-amino acid peptide: membrane lysis, increased necrosis, and inhibition of prostate-specific antigen secretion. Cancer Res 64(16):5779–5786

Shai Y (1999) Mechanism of the binding, insertion and destabilization of phospholipid bilayer membranes by alpha-helical antimicrobial and cell non-selective membrane-lytic peptides. Biochim Biophys Acta 1462(1–2):55–70

Sims PJ, Waggoner AS et al (1974) Studies on the mechanism by which cyanine dyes measure membrane potential in red blood cells and phosphatidylcholine vesicles. Biochemistry 13(16):3315–3330

Subbalakshmi C, Nagaraj R et al (1999) Biological activities of C-terminal 15-residue synthetic fragment of melittin: design of an analog with improved antibacterial activity. FEBS Lett 448(1):62–66

Suh JY, Lee YT et al (1999) Structural and functional implications of a proline residue in the antimicrobial peptide gaegurin. Eur J Biochem 266(2):665–674

Varkey J, Nagaraj R (2005) Antibacterial activity of human neutrophil defensin HNP-1 analogs without cysteines. Antimicrob Agents Chemother 49(11):4561–4566

Weber G, Shinitzky M (1970) Failure of energy transfer between identical aromatic molecules on excitation at the long wave edge of the absorption spectrum. Proc Natl Acad Sci USA 65(4):823–830

Wu CS, Ikeda K et al (1981) Ordered conformation of polypeptides and proteins in acidic dodecyl sulfate solution. Biochemistry 20(3):566–570

Yadav SP, Kundu B et al (2003) Identification and characterization of an amphipathic leucine zipper-like motif in *Escherichia coli* toxin hemolysin E. Plausible role in the assembly and membrane destabilization. J Biol Chem 278(51):51023–51034

Yadav SP, Ahmad A et al (2008) Inhibition of lytic activity of *Escherichia coli* toxin hemolysin E against human red blood cells by a leucine zipper peptide and understanding the underlying mechanism. Biochemistry 47(7):2134–2142

Yeaman MR, Yount NY (2003) Mechanisms of antimicrobial peptide action and resistance. Pharmacol Rev 55(1):27–55

Zasloff M (2002) Antimicrobial peptides of multicellular organisms. Nature 415(6870):389–395

Zhu WL, Nan YH et al (2007a) Cell selectivity of an antimicrobial peptide melittin diastereomer with D-amino acid in the leucine zipper sequence. J Biochem Mol Biol 40(6):1090–1094

Zhu WL, Song YM et al (2007b) Substitution of the leucine zipper sequence in melittin with peptoid residues affects self-association, cell selectivity, and mode of action. Biochim Biophys Acta 1768(6):1506–1517